Molecular Crystals and Liquid Crystals

Publication details, including instructions for authors and subscription information:
http://www.tandfonline.com/loi/gmcl20

Nonlinear Shape Perturbations Induced by Vesicle Inclusions

Paolo Biscari [a] & Gaetano Napoli [b]

[a] Dipartimento di Matematica, Politecnico di Milano, Piazza Leonardo da Vinci, Milano and Istituto Nazionale di Fisica della Materia, Italy

[b] Dipartimento di Matematica, Politecnico di Milano, Piazza Leonardo da Vinci, Milano, Italy

Version of record first published: 31 Jan 2007

To cite this article: Paolo Biscari & Gaetano Napoli (2005): Nonlinear Shape Perturbations Induced by Vesicle Inclusions, Molecular Crystals and Liquid Crystals, 434:1, 271/[599]-279/[607]

To link to this article: http://dx.doi.org/10.1080/15421400590956649

Mol. Cryst. Liq. Cryst., Vol. 434, pp. 271/[599]–279/[607], 2005

ISSN: 1542-1406 print/1563-5287 online
DOI: 10.1080/15421400590956649

Taylor & Francis
Taylor & Francis Group

Nonlinear Shape Perturbations Induced by Vesicle Inclusions

Paolo Biscari
Dipartimento di Matematica, Politecnico di Milano, Piazza Leonardo da Vinci, Milano and Istituto Nazionale di Fisica della Materia, Italy

Gaetano Napoli
Dipartimento di Matematica, Politecnico di Milano, Piazza Leonardo da Vinci, Milano, Italy

We analyse the effects that a rigid inclusion induces on the stationary shapes of an impermeable three-dimensional vesicle. Our study, performed via a numerical calculation, takes into account shapes which are not close to any reference configuration (neither spherical nor planar). The shape perturbations induced by the embedded inclusions are restricted within distances of the order of the inclusion size. Thus, inclusions do not interfere with global vesicle properties, such as budding transitions. The local character of the inclusion perturbation announces a fast distance decay of the membrane mediated elastic force between different proteins.

Keywords: biological membranes; inclusions; nonlinear equilibrium

1. INTRODUCTION

We study the stationary shapes of a three-dimensional impermeable vesicle hosting a rigid inclusion. The inclusion-induced perturbations modify the vesicle elastic energy, which in turn determines a membrane-mediated elastic interaction between the inclusions. This interaction has been widely studied both experimentally [1] and theoretically, in the cases of planar [2–4], quasi-planar [5,6], and

This work was made possible by the Post-Doctoral Fellowship "Mathematical Models for Fluid Membranes", supported by the Mathematical Department of the *Politecnico di Milano*.

Address correspondence to Gaetano Napoli, Dipartimento di Matematica, Politecnico di Milano, Piazza Leonardo da Vinci 32–20133 Milano, Italy. E-mail: gaetano.napoli@mate.polimi.it

quasi-spherical vesicles [7,8]. We aim at determining numerically the stationary shapes, as a first step towards the computation of the membrane-mediated force between inclusions hosted by vesicles that are not close to any reference shape. Throughout this paper we will often refer to [8], of which this paper is the continuation.

We describe the vesicle elasticity through the spontaneous curvature model [9,10]. At fixed vesicle area and enclosed volume, the effective free-energy functional to be minimized is

$$\mathcal{F}_{\text{eff}}[\Sigma] := \kappa \int_{\Sigma} (H - \sigma_0)^2 da + \lambda \left(\text{Area}\,(\Sigma) - A\right) + \mu \left(\text{Vol}\,(\Sigma) - V\right). \quad (1.1)$$

where Σ is a closed surface describing the vesicle shape, H denotes the mean curvature along Σ, κ is the bending rigidity, and σ_0 the spontaneous curvature. The Lagrange multipliers λ, μ have the physical meaning of surface tension and pressure difference. The Euler-Lagrange equation associated to (1.1) is the *shape equation* [11,12]:

$$\kappa\left[\Delta_s H + 2H\left(H^2 - K\right) + 2\sigma_0 K - 2\sigma_0^2 H\right] - 2\lambda H - \mu = 0, \quad (1.2)$$

where Δ_s, the tangential divergence of the tangential gradient, is the Laplace-Beltrami operator on Σ, and K denotes the Gaussian curvature along Σ.

We now consider a vesicle which embeds an inclusion, that we model as a symmetric conical frustum of negligible height, base radius a, and apex angle ϕ. The inclusion-vesicle interaction fixes the angle between the vesicle normal and the inclusion plane at the contact points to be equal to $(\pi/2 - \phi)$. We restrict our analysis to vesicle shapes which are axisymmetric about the inclusion axis.

To describe the surface shape we introduce the normalized arc-length[1] s along the curve which generates Σ. On the top of the vesicle we set $s = 0$, so that $s = 1$ at the contact point. To determine the stationary shapes we have solved numerically the shape Eq. (1.2). To this aim, we have introduced the tilt angle ψ, determined by the oriented tangent to the generating curve and the plane containing the inclusion [13]. The shape equation is a third order ordinary differential equation in ψ, that is to be solved also taking into account the free boundary conditions at $s = 0$ and the contact conditions at $s = 1$.

In the next Section we will describe the families of stationary shapes that can be obtained from (1.2) by varying the vesicle area and/or the

[1]The normalized arc-length is defined as the arc-length divided by the length of the curve.

enclosed volume. Section 3 focuses on the perturbations induced by the inclusion on the vesicle shape. In Section 4 we summarize and discuss our results.

2. NONLINEAR EVOLUTION OF QUASI-SPHERICAL SHAPES

In [8] the quasi-spherical stationary shapes of a vesicle hosting a rigid inclusion have been analytically determined. It has been there shown that a given modification of the inclusions and/or vesicle geometric parameters may induce shape modifications of different orders of magnitude, depending on the vesicle permeability.

In the impermeable case, the spherical solution bifurcates into a double infinity of stationary branches. In spherical coordinates, the shape function in the k-th branch can be written in terms of a Legendre function of the first kind of order ν_k:

$$r_{k\pm}(\vartheta) = r_0 \pm \epsilon \left(C_1 + C_2 \cos\vartheta + C_3 P_{\nu_k}(\vartheta)\right). \tag{2.1}$$

In (2.1), r denotes the distance from the origin (placed at the center of the sphere we perturb), ϑ is the polar angle about the inclusion axis, while C_1, C_2, C_3 are integration constants that depend on the boundary conditions (with $C_3 > 0$). The order ν_k of the Legendre function can be obtained by solving a suitable eigenvalue problem that was derived and studied in [8]. It was there shown that this eigenvalue problem admits a countable infinity of solutions $\{\nu_k,\, k \in \mathbb{N}\}$, that we can order to obtain an (unbounded) increasing sequence: $\nu_{k+1} > \nu_k$ for all $k \in \mathbb{N}$, with $\nu_1 \geq 2$. Solutions which involve higher-order Legendre functions are more and more wrinkled. They possess an increasing deformation energy. In this section we follow the shape branches while they evolve beyond the quasi-spherical regime.

In order to non-dimensionalize our equations, we define the reduced volume $\upsilon := 3\sqrt{4\pi}\, V A^{-3/2}$ and the reduced spontaneous curvature $\varsigma_0 := \sigma_0 r_\circ$, where the surface radius $r_\circ := \sqrt{A/(4\pi)}$ is the radius of a sphere having the same area of the vesicle. Whatever the surface shape, it holds $\upsilon \in [0,1]$, with the limiting cases $\upsilon = 0$ and $\upsilon = 1$ attained by planar and spherical surfaces, respectively.

Figure 1 reports the elastic free energy stored in the lower-order branches of stationary shapes for a vesicle hosting an almost negligible inclusion, *i.e.* an inclusion of almost null length and apex angle. The reduced spontaneous curvature is null in Figure 1a, while it attains positive ($\varsigma_0 = 1.5$) and negative ($\varsigma_0 = -0.9$) values in Figures 1b and 1c, respectively. Not surprisingly, Figure 1a follows quite closely the diagram reported in [13] for a free vesicle with null

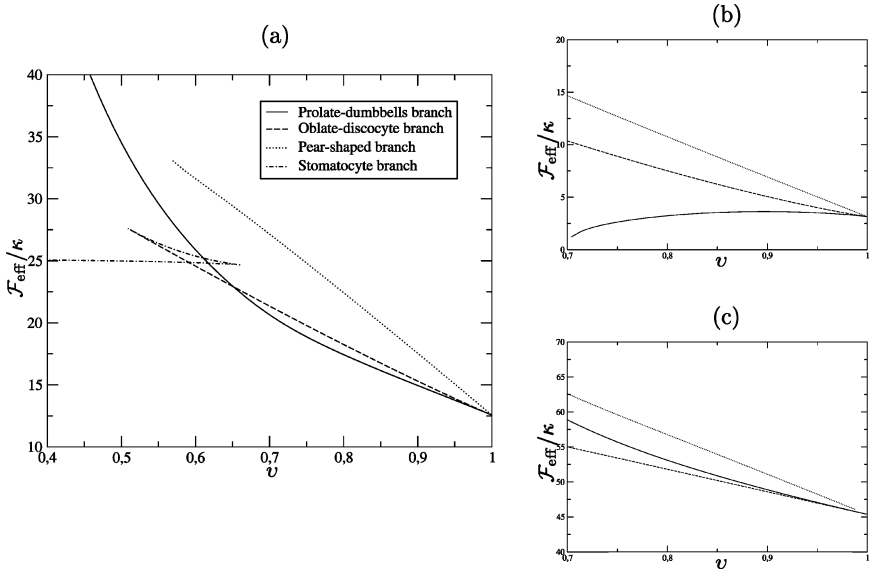

FIGURE 1 Free energy stored in the stationary shape branches when the reduced spontaneous curvature equals 0 (a), 1.5 (b), and −0.9 (c). The continuous lines always refer to prolate-dumbbells shapes; the dashed lines are the oblate-discocyte branches; the dotted lines represent pear-shaped solutions; finally, the dashed-dotted lines identify stomatocytes.

spontaneous curvature. However, we have observed that the free-energy plots remain almost unchanged even when inclusions of non negligible size and/or apex angle are taken into account – at least as long as the inclusion size a remains sensibly smaller than the surface radius $r_\circ$. In the next section we will explain why inclusions influence so weakly the global properties of the absolute minimizer of the free-energy functional.

Let us denote as Σ_{k+} (respectively, Σ_{k-}) the vesicle shape branch which bifurcates from the sphere through a shape function as in (2.1), with the k-th eigenvalue ν_k as Legendre order and the plus (resp. minus) sign in front of the perturbation. Then the prolate-dumbbells branch can be labelled as Σ_{1+}; the oblate-discocyte branch (that eventually becomes the stomatocyte branch) corresponds to Σ_{1-}. The pear-shaped branch describes both Σ_{2+} and Σ_{2-}, that share the same free energy by symmetry, as we will see below. This branch was not reported in [13], probably because it never hosts the absolute minimizer of the free-energy functional. Further branches could be identified, but their free energies increase monotonically with k. Figure 2 justifies

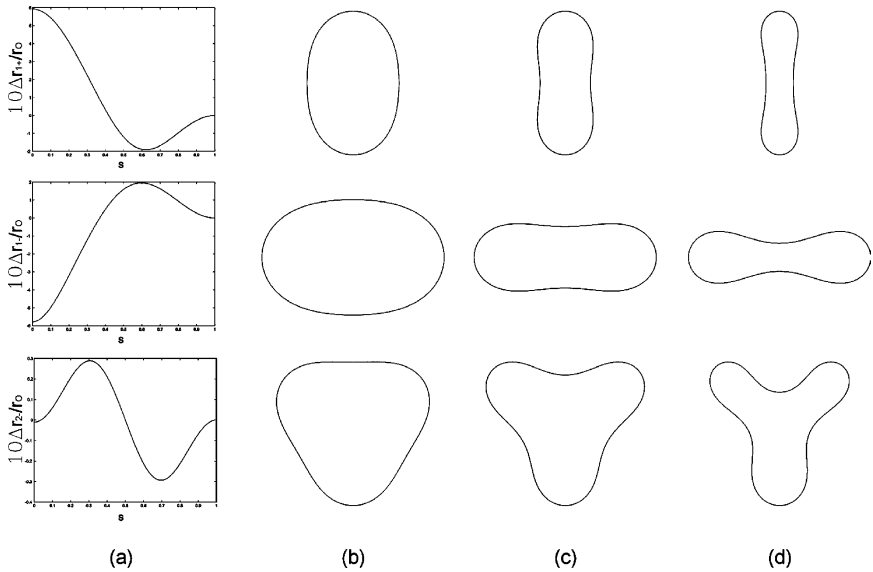

FIGURE 2 Stationary shapes for a vesicle of null spontaneous curvature, hosting an almost negligible inclusion. Column (a) shows the perturbating functions which give rise to the quasi-spherical shapes ($\upsilon = 0.95$) reported in the (b) column. When we decrease the reduced volume ($\upsilon = 0.8$ in (c); $\upsilon = 0.65$ in (d)) the stationary vesicle shapes move away from those predicted by the linearized theory [8].

the labelling chosen for every branch: in column (a) we show how the radial perturbation with respect to the spherical shape depends on the normalized arc-length; columns (b), (c), (d) show how the shapes evolve when the reduced volume decreases.

The analytical calculations reported in [8] proved that, close to the spherical solution, the absolute minimizer of the free-energy functional is always either the Σ_{1+} or the Σ_{1-} solution, depending on the reduced spontaneous curvature. More precisely, it exists a (negative) critical value of the spontaneous curvature above which Σ_{1+} is the absolute minimizer, with Σ_{1-} preferred on the opposite side. Figure 1 confirms this result. In addition, it shows that when we decrease the reduced volume the preferred branch may or may not remain unchanged.

With a null spontaneous curvature (Fig. 1a), the free-energy increases quite more rapidly along the the prolate-dumbbells branch than along the oblate-discocyte one. For $\upsilon < 0.65$, oblate-discocyte shapes become energetically favored. When we further decrease the reduced volume, these shapes self-intersect for $\upsilon \simeq 0.50$. However,

the Σ_{1-} shapes evolve continuously until they stabilize in the stomatocyte branch, which for $v < 0.59$ host the free energy minimized. As it has been already remarked in [13], these shapes have a bending energy which doubles the spherical one.

When $\varsigma_0 > 0$ (Fig. 1b), the prolate branch does never hand the absolute minimizer to the oblate one. Prolate shapes in this branch develop a neck in the middle, that eventually leads to a vesicle budding transition. For the reported value of the spontaneous curvature this transition occurs at $v \lesssim 0.70$. On the contrary, if ς_0 is sufficiently negative (Fig. 1c), prolate shapes are preferred even close to the spherical shape.

In all cases, when $v = 1 - \epsilon$, the free-energy difference between prolate and oblate shapes is much smaller than the difference between Σ_1 and Σ_2 shapes. In fact (see §4 of [8]), the difference between shapes sharing the same k value scales as $\epsilon^{3/2}$, while the energy difference between shapes corresponding to different k values scales as ϵ.

3. APEX ANGLE EFFECTS

Up to this point we have focused on the effects induced on the vesicle shape by a smooth variation of the membrane parameters (spontaneous curvature and reduced volume), while keeping fixed the inclusion parameters. In this section we address a different question: how do the stationary shapes change when the inclusion varies?

As for the inclusion size, the small $a/r_\circ$ limit is physically the only realistic one. Our numerical simulations show that no singular shape behaviour arises if we change the inclusion size a in the regime $a << r_\circ$.

More interesting effects come into play when we vary the inclusion apex angle, which is not necessary small in real inclusions. As we announced in the previous section, when the apex angle is small the presence of the inclusion does not modify the stationary shapes. In this case the tilt angle in the contact point approaches the tilt angle a free vesicle would have in the same point.

We have analysed the apex angle effects on a number of stationary shapes, obtained with several different values of ς_0 and v. For increasing values of the apex angle, the inclusion does induce vesicle distortion. However, our main observation is that, in all cases, the distortion is strongly localized, in the sense that it quickly decays along the vesicle. The presence of the inclusion does not affect the vesicle shape far away from the contact point, and the bending energy is only slightly affected. Therefore, the presence of the inclusion does not modify the complete phase diagram presented by Seifert and co-workers in [13]. We remark that the opposite result holds for planar

vesicles. In that case, the presence of an embedded inclusion induces global shape modifications, and may even wreck the existence of regular stationary shapes [3,4].

The motivation for this completely different behaviour is exactly the same that allows the existence of three-dimensional buds and avoids them in regular planar shapes. In a three-dimensional surface the mean curvature is the average between the two principal curvatures, while in a planar curve only one curvature comes into play. In the three-dimensional case, a very quick change in the normal direction is not necessarily too expensive in terms of free energy: the mean curvature may be kept bounded by averaging a large, positive, principal curvature with a second similarly large, but negative, principal curvature. The optimal minimizing strategy for a three-dimensional vesicle hosting an inclusion thus consists in keeping as close as possible to its preferred free shape, and eventually adapting locally to the inclusion contact angle with a bud-like neck.

Figure 3 confirms these predictions. In it, we compare the free shape (continuous curve labelled as "A") with shapes obtained with inclusion apex angles ϕ ranging from $\pi/20$ to $\pi/4$. The left plots confirm that the global vesicle shape is not affected neither by the presence of the inclusion nor by the value of ϕ, while the right magnifications show how the inclusion perturbation is localized close to the $s = 1$ end-point.

4. CONCLUSIONS

We have presented numerical results concerning stationary shapes of three-dimensional vesicles which host a rigid inclusion. The numerical solutions of the shape equation for reduced volumes close to the spherical value $\upsilon = 1$ confirm the analytical results for quasi-spherical vesicles derived in [8]. In the small inclusion limit, the free-energy diagrams reproduce the results obtained for a free vesicle [13].

The inclusion size, provided that it remains small, does not affect the global properties of the vesicle shape. On the contrary, when the inclusion apex angle is increased, the protein gives arise to a local distortion in the neighborhood of the contact point. This distortion decays along the vesicle contour within distances of the order of the inclusion size.

The results presented in this paper prompt two phenomena that will be subject to a more detailed investigation in a forthcoming publication.

- The local character of the perturbation induced by the inclusions suggests that the shape of the perturbation itself can be derived by a suitable perturbation method. Once the perturbation is known,

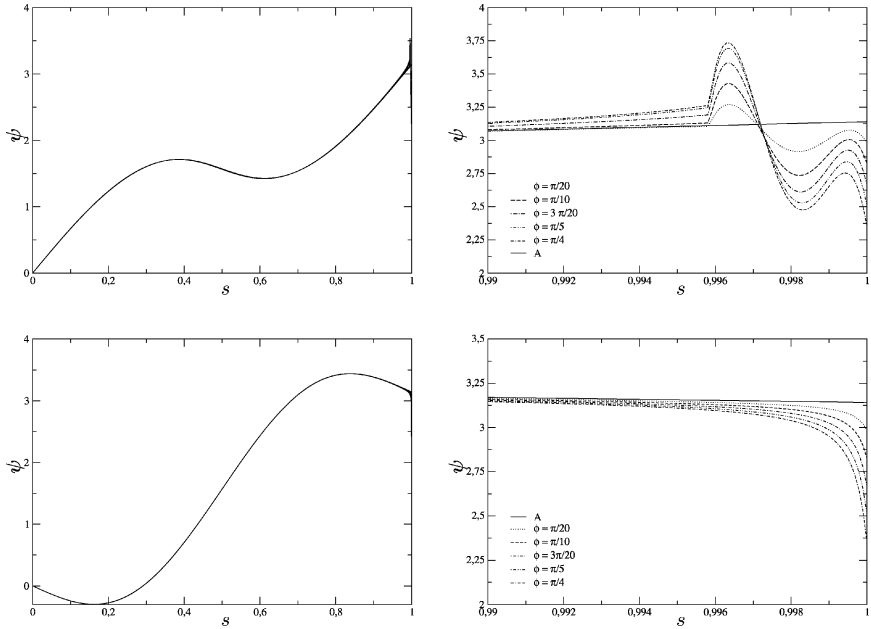

FIGURE 3 Left: dependence of the tilt angle ψ on the normalized arc-length s for a dumbbell-like shape (up, $\varsigma_0 = 1.5$, $\upsilon = 0.8$) and a discocyte-like shape (bottom, $\varsigma_0 = 0$, $\upsilon = 0.65$). Right: magnification of the left graphs, close to the contact points $s = 1$. In all the plots, the inclusion size is $a = 10^{-3} r_\circ$. Different graphs refer to different values of the inclusion apex angle ϕ (the continuous line labelled as "A" represents a free vesicle).

it is possible to compute the free-energy difference induced by the inclusion. This difference gives rise to a position-dependent potential that determines the equilibrium configurations of the inclusion along the hosting membrane.

- The perturbations induced by two (or more) inclusions are completely independent as long as their distance is greater than their size. Thus, the membrane-mediated inclusion interaction is strongly short-ranged. Once again, this is an intrinsically three-dimensional result, since the membrane-mediated interactions were proven to be long-range in the planar case [3,4].

REFERENCES

[1] Koltover, I., Rädler, J. O., & Safinya, C. R. (1999). Membrane mediated attraction and ordered aggregation of colloidal particles bound to giant phospholipid vesicles. *Phys. Rev. Lett.*, *82*, 1991–1994.

[2] Biscari, P. & Rosso, R. (2001). Inclusions embedded in lipid membranes. *J. Phys. A: Math. Gen.*, *34*, 439–459.
[3] Biscari, P., Bisi, F., & Rosso, R. (2002). Curvature effects on membrane-mediated interactions of inclusions. *J. Math. Biol.*, *45*, 37–56.
[4] Biscari, P. & Bisi, F. (2002). Membrane-mediated interactions of rod-like inclusions. *Eur. Phys. J. E*, *7*, 381–386.
[5] Goulian, M., Bruinsma, R., & Pincus, P. (1993). Long-range forces in heterogeneous fluid membranes. *Europhys. Lett.*, *22*, 145–150.
[6] Weikl, T. R., Kozlov, M. M., & Helfrich, W. (1998). Interaction of conical membrane inclusions: Effect of lateral tension. *Phys. Rev. E*, *57*, 6988–6995.
[7] Dommersnes, P. G., Fournier, J.-B., & Galatola, P. (1998). Long-range elastic forces between membrane inclusions in spherical vesicles. *Europhys. Lett.*, *42*, 233–238.
[8] Biscari, P., Canavese, S. M., & Napoli, G. (2004). Impermeability effects in three-dimensional vesicles. *J. Phys. A: Math. Gen.*, *37*, 6859–6874.
[9] Helfrich, W. (1973). Elastic properties of lipid bilayers: theory and possible experiments. *Z. Naturforsch.*, *28*, 693–703.
[10] Deuling, H. J. & Helfrich, W. (1976). The curvature elasticity of fluid membranes: A catalogue of vesicle shapes. *J. Phys. France*, *37*, 1335–1345.
[11] Zhong-Can, O.-Y. & Helfrich, W. (1987). Instability and deformation of a spherical vesicle by pressure. *Phys. Rev. Lett.*, *59*, 2486–2488.
[12] Zhong-Can, O.-Y. & Helfrich, W. (1989). Bending energy of vesicle membranes: General expressions for the first, second, and third variation of the shape energy and applications to spheres and cylinders. *Phys. Rev. A*, *39*, 5280–5288.
[13] Seifert, U., Berndl, K., & Lipowsky, R. (1991). Shape transformations of vesicles: phase diagram for spontaneous-curvature and bilayer-coupling models. *Phys. Rev. A*, *44*, 1182–1202.